Reactions of Hydrated Electrons with Pyridinium Salts in Aqueous Solutions

Kazuyuki Enomoto[†] **and Jay A. LaVerne***[,†,‡]

Radiation Laboratory and Department of Physics, University of Notre Dame, Notre Dame, Indiana 46556

Received: August 19, 2008; Revised Manuscript Received: September 22, 2008

Rate coefficients for the reactions of the hydrated electron (e_{aq}^-) with pyridinium salts in aqueous solutions have been determined using pulse radiolysis techniques. The rate coefficients for pyridine, 1-hydropyridinium chloride, and 1-hydropyridinium nitrate were observed to be 1.4×10^{10}, 4.5×10^{10}, and 5.3×10^{10} M^{-1} s^{-1}, respectively. The e_{aq}^- was found to primarily attack the pyridine ring, the proton coordinated to the nitrogen atom, and the nitrate counterion, but not the chloride. Results for the corresponding dimer structures of 4,4′-dipyridyl, 1,1′-dihydro-4,4′-bipyridinium dichloride, and 1,1′-dihydro-4,4′-bipyridinium dinitrate had similar trends for e_{aq}^- attack sites. The rate coefficients for pyridinium salts were lower when the pyridinium nitrogen atom is coordinated to a methyl group rather than to a proton. This reduction is probably due to the increase in electron density of the pyridine ring due to the electron-donating methyl group. Pyridinium salts are not major contributors to the production of molecular hydrogen in the radiolysis of aqueous solutions and actually decrease molecular hydrogen yield due to scavenging reactions of the e_{aq}^-. The yield of molecular hydrogen decreases from 0.45 to ~0.2 molecule/(100 eV) over the scavenging capacity range for the e_{aq}^- of 10^5-10^9 s^{-1}. Absorption spectra of the transient species produced by the reactions of pyridinium salts with OH radical and H atom formed in water radiolysis were observed, and rate coefficients for these reactions were determined.

Introduction

Electron-driven chemistry is a fundamental process that is an important factor in radioactive waste management, especially plutonium recovery.[1−3] Plutonium with four positive charges is the most stable oxidation state in nitric acid, forming the divalent hexanitrato complex $Pu(NO_3)_6^{2-}$.[4−6] The plutonium can be removed selectively from the nitric acid by organic polymers such as Reillex HPQ and Reillex 402, which are common anion-exchange resins.[7] Reillex HPQ is a poly(vinylpyridine)-based resin cross-linked with divinylbenzene that contains an *N*-methylpyridinium cation and nitrate (NO_3^-) or chloride (Cl^-) anions. Reillex 402 is similar, except that a proton is attached to the nitrogen. These resins are packed into a column through which the nitric acid solution is flowed, resulting in the strong retention of the divalent plutonium hexanitrato complex with two positively charged nitrogen sites of the resin. The plutonium recovery processes can lead to the formation of potentially explosive gases due to the self-radiolysis of water. Molecular hydrogen formation is especially important because enhancement of its yield can cause serious engineering and management problems.[1,8−10] Studies have examined the production of molecular hydrogen from pyridinium-based resins,[11] but little is known about the basic chemistry of this class of compounds. Fundamental kinetic information on the reactions of pyridinium salts in aqueous solutions provides mechanistic details that can be applied to other compounds containing multiple components of different reactivity.

Energy deposited by the passage of ionizing radiation in liquid water initially forms the parent water cation and a nonhydrated electron, which decays with a lifetime of 240 fs to give the hydrated electron (e_{aq}^-).[12,13] The e_{aq}^- is a strong reducing species, and it is produced with an initial yield of ~4.2 molecules/(100 eV) with γ-rays and fast electrons.[14−16] There is a reduction in the yield of e_{aq}^- to ~2.6 molecules/(100 eV) at 1 μs, primarily due to the intratrack reactions of e_{aq}^- with H_3O^+ and with OH radical.[17] The hydrated electron and its precursor are major contributors to the production of molecular hydrogen in the radiolysis of liquid water.[18]

The hydrated electron is a good nucleophile and will reduce a solute that has a positive electron affinity to give the solute anion.

$$e_{aq}^- + \text{solute} \rightarrow \text{solute}^- \tag{1}$$

Time-resolved techniques can follow this reaction by examining the formation of the anion or the loss of e_{aq}^-, which has a strong absorption at about 720 nm.[19] A large component of molecular hydrogen production is also due to reactions of the e_{aq}^-.

$$e_{aq}^- + e_{aq}^- \ (+2H_2O) \rightarrow H_2 + 2OH^- \qquad 2k_2 = 1.1 \times 10^{10}\ M^{-1}\ s^{-1} \tag{2}$$

$$e_{aq}^- + H^+ \ (+H_2O) \rightarrow H_2 + OH^- \qquad k_3 = 2.5 \times 10^{10}\ M^{-1}\ s^{-1} \tag{3}$$

The rate coefficients are taken from the compilation of Buxton et al.[19] Competition of the e_{aq}^- in reaction 1 with reactions 2 and 3 has been experimentally shown to lead to a decrease in molecular hydrogen yield.[17,18,20−26] Molecular hydrogen yields decrease with increasing solute concentrations from 0.45 to ~0.2 molecule/(100 eV) over the scavenging capacity range of 10^5-10^9 s^{-1} for the e_{aq}^-.[24] Scavenging capacities are defined as the product of the solute concentration and the scavenging rate coefficient. Reillex resins carry a pyridinium ring and the counterion, as shown in Figure 1. The former is electron-poor due to the electron-withdrawing nitrogen atom, while the latter is a good electron scavenger, especially nitrate. Knowledge of the rate coefficients for the various constituents of the solute is

---

* To whom correspondence should be addressed. E-mail: laverne.1@nd.edu.

[†] Radiation Laboratory.

[‡] Department of Physics.

10.1021/jp8074332 CCC: $40.75

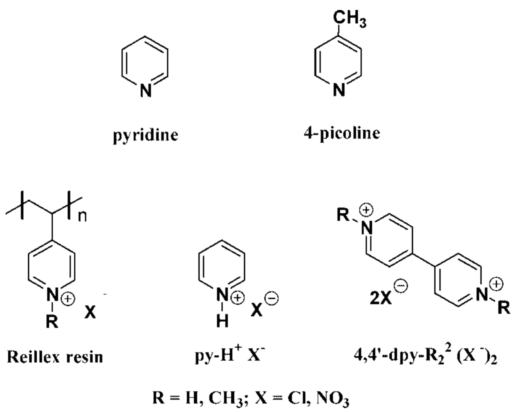

Figure 1. Structures of the pyridinium-based compounds.

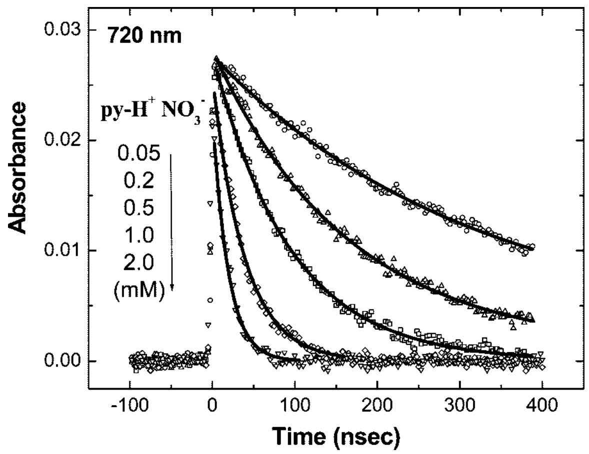

Figure 2. Kinetic decay profiles for the hydrated electron absorbance at 720 nm obtained with different concentrations of py−$H^+NO_3^-$ in deaerated aqueous solutions with 10 mM CH_3OH: (○) 0.05 mM, (Δ) 0.2 mM, (□) 0.5 mM, (◇) 1 mM, and (▽) 2 mM. The solid lines are exponential fits to the data.

needed to estimate the overall reactivity of the e_{aq}^- and to help develop radiolytic models using kinetic simulation.

In this work, rate coefficients for the reactions of e_{aq}^- with pyridinium salts in aqueous solutions were determined using pulse radiolysis techniques. OH radical and H atom reactions with pyridinium salts also were examined. The pyridinium salts were selected to mimic the Reillex HPQ and 402 resins. Molecular hydrogen yields were determined using γ-rays, and the effect of scavenging capacity for e_{aq}^- on the yield of molecular hydrogen was examined.

Experimental Section

Materials. Pyridine (HPLC grade), 4-picoline, 4,4′-dipyridyl (4,4′-dpy), and 1,1′-dimethyl-4,4′-bipyridinium dichloride (methyl viologen, 4,4′-dpy−$(CH_3)_2^{2+}(Cl^-)_2$) were from Aldrich and used without further purification. 1-Hydropyridinium chloride (py−H^+Cl^-; Aldrich) was purified by recrystallization from ethyl acetate and chloroform. All solutions were prepared using water purified by an in-house H2Only commercial system, consisting of a UV lamp and multiple micoporous filters to give a resistance of >18.2 MΩ cm and a total organic carbon content of <10 ppb.

Synthesis of the Pyridinium Salts. The salts not commercially available were prepared as follows. For the synthesis of 1-hydropyridinium nitrate (py−$H^+NO_3^-$), a solution of pyridine (0.81 mL, 10 mM) in tetrahydrofuran (THF; 25 mL) was added to HNO_3 (1.4 mL, 15 mM) at room temperature. The crystalline precipitate formed was filtered and then washed with THF (2 × 25 mL) and dried in vacuo. The solid was purified by recrystallization from methanol and chloroform to give the py−$H^+NO_3^-$ (96% yield). For the synthesis of 1,1′-dihydro-4,4′-bipyridinium dichloride (4,4′-dpy−$H_2^{2+}(Cl^-)_2$), a solution of 4,4′-dipyridyl (0.31 g, 2.0 mM) in THF (25 mL) was added to HCl (0.40 mL, 4.8 mM) at room temperature. The crystalline precipitate formed was worked up in a manner similar to that above to give the 4,4′-dpy−$H_2^{2+}(Cl^-)_2$ (94% yield). For the synthesis of 1,1′-dihydro-4,4′-bipyridinium dinitrate (4,4′-dpy−$H_2^{2+}(NO_3^-)_2$) a solution of 4,4′-dipyridyl (0.31 g, 2.0 mM) in THF (25 mL) was added to HNO_3 (0.44 mL, 4.8 mM) at room temperature. The crystalline precipitate formed was worked up in a manner similar to that above to give the 4,4′-dpy−$H_2^{2+}(Cl^-)_2$ (97% yield).

Pulse Radiolysis. Pulse-radiolysis experiments were performed using 8 MeV electrons from the Notre Dame Radiation Laboratory Q-band linear accelerator (TB-8/16-1S linac). Details of the linac, the spectrophotometric detection setup, and the computer-controlled data acquisition and detection systems are described elsewhere.[27] Dosimetry was performed with N_2O-saturated 10 mM SCN^- solutions using the following parameters for the observed $(SCN)_2^-$: $\lambda = 472$ nm, $\varepsilon = 7580$ M^{-1} cm^{-1}, $G = 6.14$ molecules/(100 eV). KSCN (Aldrich) was of the highest purity commercially available and used as received. The pulsed electron beam width was 5 ns with a dose of 6.0 Gy/pulse as determined by the thiocyanate dosimeter. All measurements were performed at 20 °C in a quartz cell of 1 cm optical path length. The solutions were degassed with ultrahigh-purity argon. Transient absorption data and kinetic traces were averaged over six pulses. Analysis of the optical absorption time dependence was performed using ORIGIN (Microcal Software, Inc.) software.

γ-Radiolysis. Irradiations of aqueous pyridinium salts were performed using a Shepherd 109-68 ^{60}Co γ-source in the Radiation Laboratory at the University of Notre Dame. The dose rate was 100 Gy/min (10 krad/min) as determined using the Fricke dosimeter. [28]

GC Analysis. Molecular hydrogen was determined using an inline gas chromatography (GC) technique as previously reported.[20] The instrument was an SRI 8610 equipped with a thermal conductivity detector. The column was a 6.4 mm diameter 13X molecular sieve 3 m long, maintained at 40 °C. The sample cell was made from a quartz cuvette and contained 4.0 mL of sample. The sample was purged with ultrahigh-purity argon for 10 min at room temperature, and the cell was sealed with a four-way valve during the radiolysis. The initial concentration of pyridinium salts was 0.01−100 mM. Dose-dependent studies were performed with 0.5−2 kGy (50−200 krad). Following irradiation, the sample cell was opened to the column gas stream using the four-way valve. Calibration was performed by injection of pure hydrogen gas.

Radiation chemical yields, *G*-values, are given in units of molecules (radicals and excited spices) formed (or decayed) per 100 eV of total energy absorption.

Results and Discussion

Hydrated Electron Reactions. The transient absorption of e_{aq}^- in the electron pulse radiolysis of deaerated water is observed at about 720 nm. In neat water, the e_{aq}^- decays with a rate determined by its reactions with sibling radicals.[19] The change in the rate of decay of the e_{aq}^- absorption with an added solute can be used to determine the associated rate coefficient for the scavenging reaction. Figure 2 shows the decay profiles

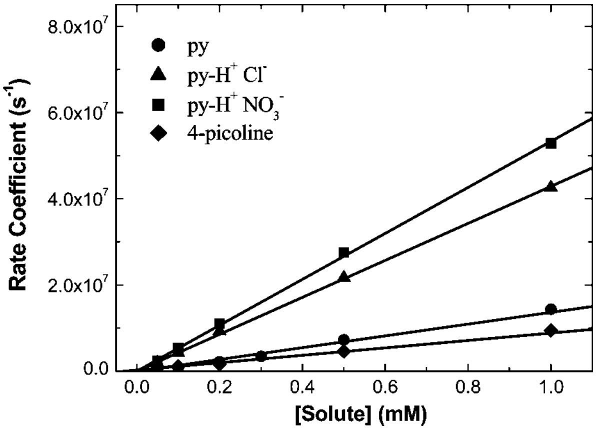

Figure 3. Pseudo-first-order rate coefficients for the e_{aq}^- reactions as a function of solute concentrations for monomer compounds: (●) pyridine, (▲) py−H^+Cl^-, (■) py−$H^+NO_3^-$, and (◆) 4-picoline.

for the e_{aq}^- absorbance at 720 nm obtained in the pulse radiolysis of different concentrations of py−$H^+NO_3^-$ in deaerated aqueous solutions of 10 mM CH_3OH at neutral pH. The e_{aq}^- absorbance exhibits first-order decay with a rate that increases linearly with increasing py−$H^+NO_3^-$ concentration. Similar results are found for pyridine, py−H^+Cl^-, and 4-picoline.

Figure 3 shows a plot of the pseudo-first-order rate coefficients for the e_{aq}^- reactions as a function of solute concentration for pyridine, py−H^+Cl^-, py−$H^+NO_3^-$, and 4-picoline. The rate coefficient for the e_{aq}^- reaction with pyridine is observed to be 1.4×10^{10} M^{-1} s^{-1}. On the other hand, the rate coefficient decreases to 8.6×10^9 M^{-1} s^{-1} for the e_{aq}^- reaction with 4-picoline, which has a methyl group at the 4-position of the pyridine ring. The decreased reaction rate is due to the increase in electron density of the pyridine ring by having an electron-donating methyl group at the 4-position. The rate coefficients for the 1-hydropyridinium salts are observed to be 4.5×10^{10} and 5.3×10^{10} M^{-1} s^{-1} for py−H^+Cl^- and py−$H^+NO_3^-$, respectively. These values are considerably greater than that for pyridine. In addition to the pyridine ring, these compounds have additional proton (coordinated to the nitrogen atom) and counterion nucleophile sites for the approach of the e_{aq}^-. The contribution of each of these sites to the overall rate coefficient can be determined separately.

A reaction involving a solute with multiple components can be analyzed in terms of the contributions of the different constituents if they react independently of each other and the overall rate is not diffusion controlled. An example will be taken as the reaction of the e_{aq}^- with py−H^+X^- (X = counterion, chloride or nitrate). The e_{aq}^- can react with three possible sites: the pyridine ring (4a), the proton (coordinated to the nitrogen atom) (4b), and the counterion (4c).

$$e_{aq}^- + \text{py}{-}H^+X^- \approx e_{aq}^- + \text{py} + \tag{4a}$$

$$e_{aq}^- + H^+ + \tag{4b}$$

$$e_{aq}^- + X^- \tag{4c}$$

Thus, the reaction kinetics of eq 4 is estimated by the simple sum of three rate coefficients.

$$-\frac{d}{dt}[e_{aq}^-] = k_{4a}[e_{aq}^-][\text{py}] + k_{4b}[e_{aq}^-][H^+] + k_{4c}[e_{aq}^-][X^-] \tag{5}$$

Since each of the components are present in the same concentration, the measured or observed rate coefficient, k_{obs} (= k_4), can be approximated by an estimated rate coefficient, k_{estd},

$$k_{obs} \approx k_{4a} + k_{4b} + k_{4c} = k_{estd} \tag{6}$$

where k_{4a} is taken as the measured rate coefficient for pyridine (1.4×10^{10} M^{-1} s^{-1}). The rate coefficients of k_{4b} and k_{4c} can be assumed to be equivalent to the reactivity of the e_{aq}^- for these nucleophiles in isolated solutions, i.e., k_7 and k_8, respectively.

$$e_{aq}^- + H^+ \rightarrow H^\bullet \quad k_7 = 2.3 \times 10^{10}\ M^{-1}\ s^{-1} \tag{7}$$

$$e_{aq}^- + NO_3^- \rightarrow NO_3^{2-} \quad k_8 = 9.7 \times 10^9\ M^{-1}\ s^{-1} \tag{8}$$

The rate coefficients k_7 and k_8 are taken from the compilation of Buxton et al.[19] The reaction of e_{aq}^- with chloride (Cl^-) has a rate coefficient of $<1.0 \times 10^6$ M^{-1} s^{-1} and can be neglected.[29] The e_{aq}^- seems to attack at two possible sites of py−H^+Cl^- (because the chloride is negligible) and at three sites of py−$H^+NO_3^-$, with estimated rate coefficients of 3.7×10^{10} and 4.7×10^{10} M^{-1} s^{-1}, respectively. The estimation is the simple sum of three rate coefficients of k_{obs} (py), k_7 (H^+), and k_8 (NO_3^-). The measured rate coefficients for py−H^+Cl^- and py−$H^+NO_3^-$ of 4.5×10^{10} and 5.3×10^{10} M^{-1} s^{-1}, respectively, agree closely with the estimated rate coefficients, suggesting that the assumption of a sum of simple nucleophile reactions of the e_{aq}^- toward the separate components in the pyridinium salts is reasonably valid.

Methyl viologen has been extensively studied and is known to be a good scavenger of e_{aq}^-, H atom, and OH radical giving a radical cation. [30−33] The kinetics of the similar structured dihydropyridinium salts, 4,4′-dpy−$H_2^{2+}(Cl^-)_2$ and 4,4′-dpy−$H_2^{2+}(NO_3^-)_2$, are not known. Figure 4 shows a plot of the pseudo-first-order rate coefficients for the e_{aq}^- reactions as a function of solute concentration in deaerated aqueous solutions with 10 mM CH_3OH at neutral pH, and the corresponding second-order rate coefficients are given in Table 1. The e_{aq}^- absorbance at 720 nm exhibits a first-order decay for all solutes. The observed rate coefficient for the e_{aq}^- reaction with 4,4′-dpy is 3.2×10^{10} M^{-1} s^{-1}, which agrees well with previous

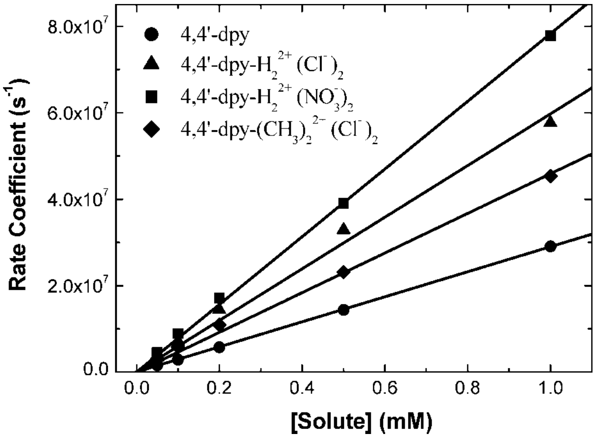

Figure 4. Pseudo-first-order rate coefficients for the e_{aq}^- reactions as a function of solute concentrations for dimer compounds: (●) 4,4′-dpy, (▲) 4,4′-dpy−$H_2^{2+}(Cl^-)_2$, (■) 4,4′-dpy−$H_2^{2+}(NO_3^-)_2$, and (◆) 4,4′-dpy−$(CH_3)_2^{2+}(Cl^-)_2$.

TABLE 1: Rate Coefficients of Pyridinium-Based Compounds with the Hydrated Electron, Hydrogen Atom, and Hydroxyl Radical

			e_{aq}^-		H	OH
compound	R	X	$k_{obs} \times 10^{-10}$, M^{-1} s^{-1}	$k_{estd} \times 10^{-10}$, M^{-1} s^{-1}	$k \times 10^{-9}$, M^{-1} s^{-1}	$k \times 10^{-8}$, M^{-1} s^{-1}
pyridine			1.4			
4-picoline			0.86			
$py^+{-}HX^-$		Cl	4.5	3.7		
		NO_3	5.3	4.7		
4,4′-dpy	–	–	3.2	2.8	0.20[a]	53[a]
4,4′-dpy$-R_2^{2+}(X^-)_2$	H	Cl	6.5	7.4	1.1	0.16
	H	NO_3	8.6	9.3	1.0	0.15
	CH_3	Cl	5.9		0.25	1.4

[a] Reference 35.

reports[34,35] and is essentially twice that for pyridine (1.4×10^{10} M^{-1} s^{-1}). This result suggests that each pyridine ring of 4,4′-dpy is an independent site for the e_{aq}^- attack. The rate coefficients for 4,4′-dpy$-H_2^{2+}(Cl^-)_2$ and 4,4′-dpy$-H_2^{2+}(NO_3^-)_2$ are observed to be 6.5×10^{10} and 8.6×10^{10} M^{-1} s^{-1}, respectively. The e_{aq}^- would be expected to react at four possible sites of 4,4′-dpy$-H_2^{2+}(Cl^-)_2$ (because the chloride is negligible) and at six sites of 4,4′-dpy$-H_2^{2+}(NO_3^-)_2$, with estimated rate coefficients of 7.4×10^{10} and 9.3×10^{10} M^{-1} s^{-1}, respectively, as listed in Table 1. The agreement between the observed and estimated rate coefficients is good, but with some noticeable differences. The observed rate coefficients are slightly lower than expected, which is probably due to stereometric effects because of the large size of the solutes and the diffusion limit. Diffusion is the ultimate rate determining process, and the summation of the rate coefficients for individual constituents cannot exceed the diffusion limited rate coefficient. The results observed here are somewhat surprising in that additivity seems to hold for rates very near to the diffusion limit and for reaction sites that are physically close to each other. These observations are not necessarily applicable to other compounds.

The observed rate coefficient for the reaction of e_{aq}^- with methyl viologen, 4,4′-dpy$-(CH_3)_2^{2+}(Cl^-)_2$, is found to be 5.9×10^{10} M^{-1} s^{-1}, in good agreement with previous reports.[32,36,37] This rate coefficient is closer to the rate coefficient for 4,4′-dpy$-H_2^{2+}(Cl^-)_2$ than for 4,4′-dpy$-H_2^{2+}(NO_3^-)_2$ because of the lack of contribution from the Cl^- groups. The rate coefficient for 4,4′-dpy$-(CH_3)_2^{2+}(Cl^-)_2$ is slightly less than that for 4,4′-dpy$-H_2^{2+}(Cl^-)_2$ because of the electron-donating nature of the methyl group. A similar effect was observed between pyridine and 4-picoline.

Molecular Hydrogen Production. The e_{aq}^- is a major contributor to the production of molecular hydrogen in the radiolysis of liquid water. [20,23−26] Figure 5 shows the yield of molecular hydrogen as a function of the scavenging capacity for each of the pyridine-based compounds in the radiolysis of liquid water with γ-rays. Also shown are the results with NO_3^- obtained in a previous work. [20] The scavenging capacity for the pyridinium salts is the product of the solute concentration and the associated scavenging rate coefficient from Table 1. The lifetime of the e_{aq}^- is approximately equal to the inverse of the scavenging capacity. With increasing scavenging capacity, the yields of molecular hydrogen decrease because a smaller amount of e_{aq}^- is available for its production. The agreement between the results for the pyridine-based compounds and that for NO_3^- suggests that a simple scavenging mechanism is valid and that very little H_2 is formed directly from the pyridinium salts. Previous studies with neat pyridine found a yield of H_2 of 0.027 molecule/(100 eV).[38] Dry Reillex HPQ resins have yields of H_2 of only 0.066 and 0.047 molecule/(100 eV) for the chloride and nitrate forms, respectively.[11] Similar small values are expected for the other pyridine-based salts, suggesting that in aqueous solutions they act mainly as e_{aq}^- scavengers and not major sources of H_2.

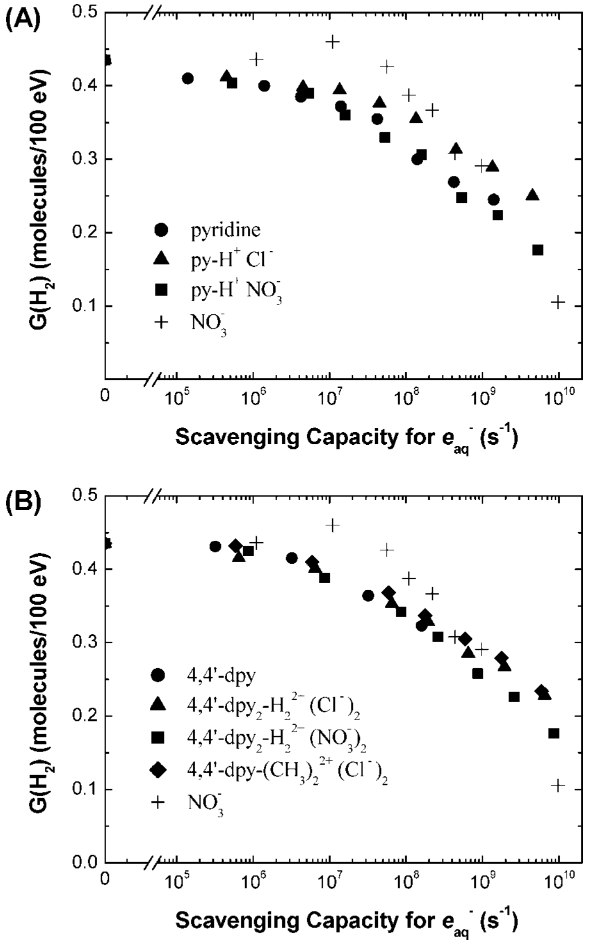

Figure 5. Molecular hydrogen yields as a function of the e_{aq}^- scavenging capacity: (A) scavenger experiments for the monomers (●) pyridine, (▲) $py{-}H^+Cl^-$, and (■) $py{-}H^+NO_3^-$; (B) scavenger experiments for the dimers (●) 4,4′-dpy, (▲) 4,4′-dpy$-H_2^{2+}(Cl^-)_2$, (■) 4,4′-dpy$-H_2^{2+}(NO_3^-)_2$, and (◆) 4,4′-dpy$-(CH_3)_2^{2+}(Cl^-)_2$, (+) NO_3^- (these NO_3^- data from ref 20).

Transient Spectra. Figure 6 shows the observed transient absorption spectra in the pulse radiolysis of deaerated aqueous solutions of 5 mM 4,4′-dpy, 4,4′-dpy$-H_2^{2+}(Cl^-)_2$, 4,4′-dpy$-H_2^{2+}(NO_3^-)_2$, and 4,4′-dpy$-(CH_3)_2^{2+}(Cl^-)_2$ at natural pH. The 4,4′-dpy involves the capture of e_{aq}^- formed from the

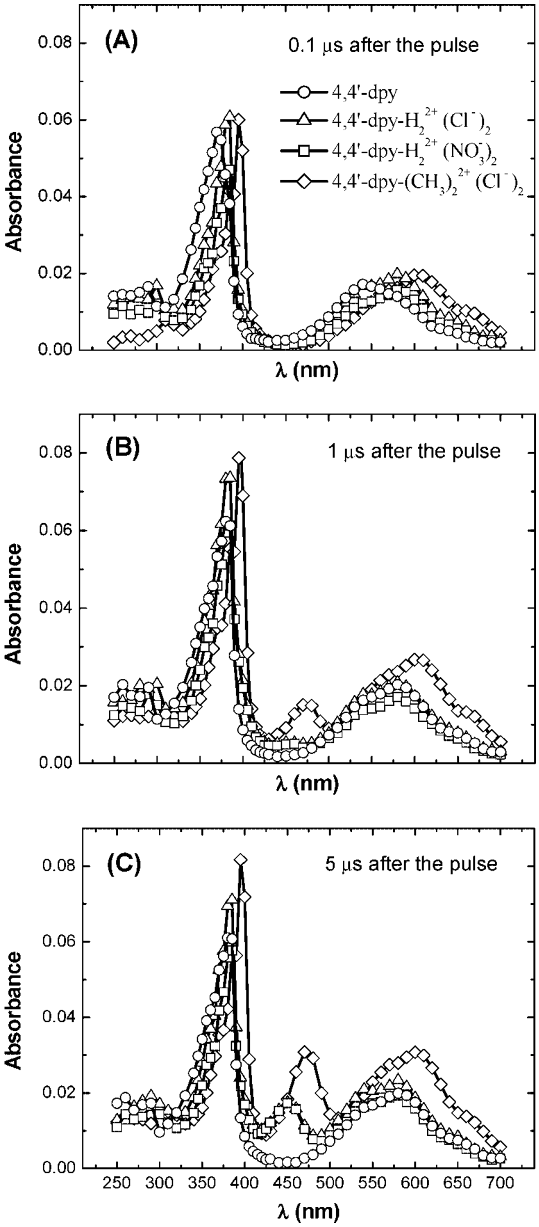

Figure 6. Transient absorption spectra observed in the pulse radiolysis of deaerated aqueous solutions of 5 mM (○) 4,4′-dpy, (Δ) 4,4′-dpy−$H_2^{2+}(Cl^-)_2$, (□) 4,4′-dpy−$H_2^{2+}(NO_3^-)_2$, and (◇) 4,4′-dpy−$(CH_3)_2^{2+}(Cl^-)_2$ at natural pH conditions at (A) 0.1, (B) 1, and (C) 5 *μ*s after the pulse.

decomposition of water to give the radical anion 4,4′-dpy$^{\bullet-}$. The protonation reaction of the 4,4′-dpy$^{\bullet-}$ with H^+ then occurs immediately, giving the monohydro radical 4,4′-dpy−H$^\bullet$, which has been assigned λ_{max} = 370 and 560 nm.[39−45]

$$e_{aq}^- + 4{,}4'\text{-dpy} \rightarrow 4{,}4'\text{-dpy}^{\bullet-} \qquad (9)$$

$$4{,}4'\text{-dpy}^{\bullet-} + H_2O \rightarrow 4{,}4'\text{-dpy-H}^\bullet + OH^- \qquad (10)$$

At 0.1 *μ*s after the pulse (Figure 6a), the absorption bands of 4,4′-dpy−H$^\bullet$ are observed at 370 and 560 nm, which agree well with the previous studies of Poizat et al.[41−45] On the other hand, at 1 *μ*s after the pulse (Figure 6b) the observed absorption bands of 4,4′-dpy−H$^\bullet$ are sifted to longer wavelengths at 375 and 580 nm. The 4,4′-dpy−H$^\bullet$ formed at 0.1 *μ*s after the pulse seems to coordinate with the water (N•••H−OH) to give the dihydro radical cation 4,4′-dpy−$H_2^{\bullet+}$, which is assigned λ_{max} = 375 and 580 nm and has attained equilibrium by 5 *μ*s after the pulse (Figure 6c).[34,41−45]

$$4{,}4'\text{-dpy-H}^\bullet \cdot\cdot\cdot \text{H−OH} \leftrightarrows 4{,}4'\text{-dpy−H}_2^{\bullet+} + OH^- \qquad (11)$$

Thus, the absorption bands at 375 and 580 nm can be assigned to the 4,4′-dpy−$H_2^{\bullet+}$.

As expected, the reaction of e_{aq}^- with the dimer salts (4,4′-dpy−$H_2^{2+}(Cl^-)_2$ and 4,4′-dpy−$H_2^{2+}(NO_3^-)_2$) gives a reduced transient (4,4′-dpy−$H_2^{\bullet+}$, dihydro radical cation) due to a one-electron reduction similar to that for 4,4′-dpy. At 0.1 *μ*s after the pulse (Figure 6a), the absorption bands for 4,4′-dpy−$H_2^{2+}(Cl^-)_2$ and 4,4′-dpy−$H_2^{2+}(NO_3^-)_2$ appear at 375 and 580 nm, respectively, which closely agree with that observed for the 4,4′-dpy−$H_2^{\bullet+}$. Furthermore, at 5 *μ*s after the pulse (Figure 6c) the absorption spectra of 4,4′-dpy, dpy−$H_2^{2+}(Cl^-)_2$ and dpy−$H_2^{2+}(NO_3^-)_2$ are nearly identical. Figure 7 shows the time profiles recorded at 375 and 720 nm in the pulse radiolysis of deaerated aqueous solutions of 0.5 mM 4,4′-dpy−H_2^{2+}-$(NO_3^-)_2$ in the presence of 10 mM CH_3OH at natural pH. Radical cation formation occurs concomitantly with e_{aq}^- decay. The rate coefficient for the formation of the radical cation of 4,4′-dpy−$H_2^{2+}(NO_3^-)_2$ was determined from a fit to the radical cation formation profile at 375 nm to be 3.5 × 10^{10} M^{-1} s^{-1}, which agrees well with the observed rate coefficient for the decay of e_{aq}^- with 4,4′-dpy, k_{obs} = 3.2 × 10^{10} M^{-1} s^{-1}. This agreement suggests that the formation of dpy−$H_2^{\bullet+}$ radical cation is due to the e_{aq}^- reactions with the dipyridyl rings of 4,4′-dpy−$H_2^{2+}(NO_3^-)_2$ and not with the proton (coordinated to the nitrogen atom) or the nitrate constituents. The rate coefficient for the decay of the electron at 720 nm in Figure 7 (8.6 × 10^{10} M^{-1} s^{-1}) is much faster than the radical cation formation rate because the electron can react with the proton (coordinated to the nitrogen atom) and the nitrate constituents.

The reaction of e_{aq}^- with 4,4′-dpy−$(CH_3)_2^{2+}(Cl^-)_2$ gives the 4,4′-dpy−$(CH_3)_2^{\bullet+}$ dimethyl radical cation, which possesses two absorption bands at 393 and 600 nm.[32] At 0.1 *μ*s after the pulse (Figure 6a), the absorption bands for 4,4′-dpy−$(CH_3)_2^{2+}(Cl^-)_2$ are observed at 390 and 600 nm in agreement with the literature.[32] The two absorption bands of 4,4′-dpy−$(CH_3)_2^{2+}$-$(Cl^-)_2$ appear at longer wavelengths than those of 4,4′-dpy−$H_2^{\bullet+}$ (λ_{max} = 375 and 580 nm) and 4,4′-dpy−H$^\bullet$ (λ_{max} = 370 and 560 nm), indicating that the stability of the dipyridyl ring systems is on the order of 4,4′-dpy−$(CH_3)_2^{\bullet+}$ > 4,4′-dpy−$H_2^{\bullet+}$ > 4,4′-dpy−H$^\bullet$.

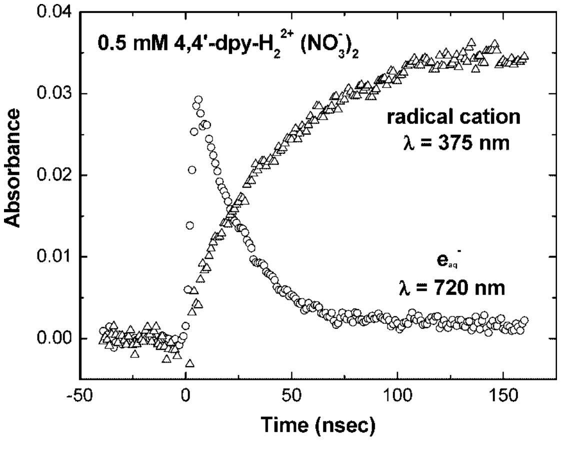

Figure 7. Time profiles recorded at (Δ) 375 nm and (○) 720 nm in the pulse radiolysis of deaerated aqueous 0.5 mM 4,4′-dpy−$H_2^{2+}(NO_3^-)_2$ in the presence of 10 mM CH_3OH at natural pH conditions.

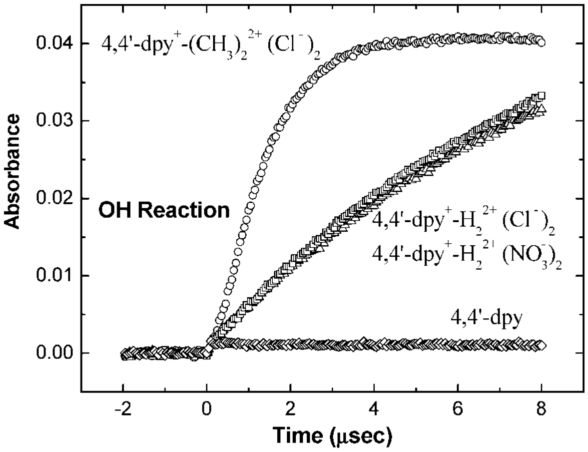

Figure 8. Time profiles of the •OH adducts formed in the pulse radiolysis of N_2O saturated aqueous 5 mM solutions at natural pH of (Δ) 4,4′-dpy−-$H_2^{2+}(Cl^-)_2$ at 450 nm, (□) 4,4′-dpy−$H_2^{2+}(NO_3^-)_2$ at 450 nm, (○) 4,4′-dpy−$(CH_3)_2^{2+}(Cl^-)_2$ at 470 nm, and (◇) 4,4′-dpy at 450 nm.

Hydroxyl Radical and H Atom Reactions. Hydroxyl radicals are the predominant oxidizing species produced in water radiolysis with a yield of 2.7 radicals/(100 eV).[46] Hydroxyl radical reactions with aromatics mainly lead to the formation of adducts, which could lead to structural damage to the pyridinium salts causing changes in the physical and chemical properties of reprocessing systems employing these salts.

Pulse radiolysis techniques were used to examine the formation kinetics of OH radical adducts in the pyridinium salts. The oxidation of 4,4′-dpy−$(CH_3)_2^{2+}(Cl^-)_2$ leads to the formation of the radical cation 4,4′-dpy−$(CH_3)_2OH^{\bullet+}$ with an absorption band at $\lambda_{max} = 470$ nm,[30,32] which is shown in Figure 6b at 1 μs after the pulse. At 5 μs after the pulse (Figure 6c), new absorption bands are observed for 4,4′-dpy−$H_2^{2+}(Cl^-)_2$ and 4,4′-dpy−$H_2^{2+}(NO_3^-)_2$ at 450 nm, which can be assigned to the 4,4′-dpy−$_2OH$ $^{\bullet+}$ adducts. Figure 8 shows the time profiles of the OH radical adducts formed in the pulse radiolysis of N_2O-saturated aqueous solutions of 5 mM 4,4′-dpy−$H_2^{2+}(Cl^-)_2$, 4,4′-dpy−$H_2^{2+}(NO_3^-)_2$, and 4,4′-dpy−$(CH_3)_2^{2+}(Cl^-)_2$ at natural pH conditions. The solutions were saturated with N_2O to convert the e_{aq}^- to OH radicals with a rate coefficient of 9.1×10^9 M^{-1} s^{-1}.[19,33] The reaction of OH radicals with 4,4′-dpy has been reported elsewhere.[35] The formation rate coefficients for the OH radical adducts of 4,4′-dpy−$H_2^{2+}(Cl^-)_2$ and 4,4′-dpy−H_2^{2+}-$(NO_3^-)_2$ are observed to be 1.6×10^7 and 1.5×10^7 M^{-1} s^{-1}, respectively (Table 1). The chloride and nitrate anions are poor scavengers of OH radical, and similar rate coefficients for the two salts are expected.

The rate coefficient for formation of the OH radical adduct with 4,4′-dpy−$(CH_3)_2^{2+}(Cl^-)_2$ is observed to be 1.4×10^8 M^{-1} s^{-1} (Table 1), which is about half of the value of 2.5×10^8 M^{-1} s^{-1} previously reported. [30,32] No reason for the discrepancy is known, but both values are considerably higher than the rate coefficient with 4,4′-dpy−$H_2^{2+}(Cl^-)_2$ and 4,4′-dpy−H_2^{2+}-$(NO_3^-)_2$. OH radical adduct formation is about 1 order of magnitude higher when the pyridinium nitrogen atom is coordinated to the methyl group instead of a proton. This result is probably due to the large increase in electron density of the pyridine ring with the attached electron-donating methyl group. On the other hand, H atoms formed in water radiolysis are found to react with 4,4′-dpy−$(CH_3)_2^{2+}(Cl^-)_2$ to give the 4,4′-dpy−$(CH_3)_2$ H $^{\bullet+}$ ($\lambda = 310$ nm) with a formation rate coefficient of 2.5×10^8 M^{-1} s^{-1}, which agrees with previous studies.[30,32] The rate coefficient for H atoms is 1 order of magnitude lower than that with OH radicals. For 4,4′-dpy−$H_2^{2+}(Cl^-)_2$ and 4,4′-dpy−$H_2^{2+}(NO_3^-)_2$, the formation rate coefficients of H atom adducts are observed to be 1.1×10^9 and 1.0×10^9 M^{-1} s^{-1}, respectively, which are 1 order of magnitude higher compared with OH radical reactions (Table 1). The formation kinetics of these latter two adducts were recorded at 310 nm. The electron density modification of the pyridine ring with the methyl group has completely opposite effects for OH radicals and for H atoms.

Conclusions

Rate coefficients for the reactions of e_{aq}^- with pyridinium salts in aqueous solutions have been determined using pulse radiolysis techniques. The rate coefficients for pyridine and 1-hydropyridinium salts (py−H^+Cl^- and py−$H^+NO_3^-$) were observed to be 1.4×10^{10}, 4.5×10^{10}, and 5.3×10^{10} M^{-1} s^{-1}, respectively. The e_{aq}^- was found to attack the pyridine ring and the proton (coordinated to the nitrogen atom) and the nitrate counterion but not the chloride. Similar results were also observed for the rate coefficients of the corresponding dimer structures of 4,4′-dpy, 4,4′-dpy−$H_2^{2+}(Cl^-)_2$, and 4,4′-dpy−$H_2^{2+}(NO_3^-)_2$. The rate coefficient for the reactions of e_{aq}^- with pyridinium salts was lower when the pyridinium nitrogen atom is coordinated to the methyl group rather than to a proton, which is probably due to the increase in electron density of the pyridine ring by the electron-donating methyl group. The yield of molecular hydrogen decreases from 0.45 to ~0.2 molecule/(100 eV) over the scavenging capacity range of the e_{aq}^- of 10^5−10^9 s^{-1}. Molecular hydrogen formation by the direct decomposition of the pyridinium salts is not significant, and they mainly scavenge the e_{aq}^- precursor to H_2 formation. The absorption spectra of the transient species formed by the reactions of pyridinium salts with OH radical and H atom were observed, and rate coefficients for adduct formation were determined.

Acknowledgment. The research described herein was supported by the Office of Basic Energy Sciences of the U.S. Department of Energy. This contribution is NDRL- 4773 from the Notre Dame Radiation Laboratory.

References and Notes

(1) Haschke, J. M.; Allen, T. H.; Morales, L. A. *Science* **2000**, *287*, 285.

(2) Ahearne, J. F. *Phys. Today* **1997**, *50*, 24.

(3) *DOE Standard "Stabilization, Packaging, and Storage of Plutonium-Bearing Materials"*; DOE-STD-3013-2004; U. S. Department of Energy: Washington, DC, 2004.

(4) Allen, P. G.; Veirs, D. K.; Conradson, S. D.; Smith, C. A.; Marsh, S. F. *Inorg. Chem.* **1996**, *35*, 2841.

(5) Clark, D. L.; Hobart, D. E.; Neu, M. F. *Chem. Rev.* **1995**, *95*, 25.

(6) Ryan, J. L. *J. Phys. Chem.* **1960**, *64*, 1375.

(7) Marsh, S. F. *Solvent Ext. Ion Exch.* **1989**, *7*, 889.

(8) Stock, L. M. *The Chemistry of Flammable Gas Generation*, RPP-6664, Rev. 1; CH2M HILL Hanford Group: Richland, WA, 2001.

(9) Gephart, R. E.; Lungren, R. E. *Hanford Tank Clean Up: A Guide to Understanding the Technical Issues*, PNNL-10773; Pacific Northwest National Laboratory: Richland, WA, 1995.

(10) Jonah, C. D.; Kapoor, S.; Matheson, M. S.; Mulac, W. A.; Meisel, D. *Gas Generation from Hanford Grout Samples*, 94−7; Argonne National Laboratory: Argonne, IL, 1994.

(11) Enomoto, K.; La Verne, J. A.; Tandon, L.; Enriquez, A. E.; Matonic, J. H. *J. Nucl. Mater.* **2008**, *373*, 103.

(12) Garrett, B. C.; Dixon, D. A.; Camaioni, D. M.; Chipman, D. M.; Johnson, M. A.; Jonah, C. D.; Kimmel, G. A.; Miller, J. H.; Rescigno, T. N.; Rossky, P. J.; Xantheas, S. S.; Colson, S. D.; Laufer, A. H.; Ray, D.; Barbara, P. F.; Bartels, D. M.; Becker, K. H.; Bowen, K. H.; Bradforth, S. E.; Carmichael, I.; Coe, J. V.; Corrales, L. R.; Cowin, J. P.; Dupuis, M.; Eisenthal, K. B.; Franz, J. A.; Gutowski, M. S.; Jordan, K. D.; Kay, B. D.; LaVerne, J. A.; Lymar, S. V.; Madey, T. E.; McCurdy, C. W.; Meisel, D.; Mukamel, S.; Nilsson, A. R.; Orlando, T. M.; Petrik, N. G.; Pimblott, S. M.;

Rustad, J. R.; Schenter, G. K.; Singer, S. J.; Tokmakoff, A.; Wang, L.-S.; Wittig, C.; Zwier, T. S. *Chem. Rev.* **2005**, *105*, 355.

(13) Pommeret, S.; Antonetti, A.; Gauduel, Y. *J. Am. Chem. Soc.* **1991**, *113*, 9105.

(14) Pimblott, S. M.; LaVerne, J. A.; Bartels, D. M.; Jonah, C. D. *J. Phys. Chem.* **1996**, *100*, 9412.

(15) Bartels, D. M.; Gosztola, D.; Jonah, C. D. *J. Phys. Chem. A* **2001**, *105*, 8069.

(16) Muroya, Y.; Lin, M. Z.; Wu, G. Z.; Lijima, H.; Yoshi, K.; Ueda, T.; Kudo, H.; Katsumura, Y. *Radiat. Phys. Chem.* **2005**, *72*, 169.

(17) Pimblott, S. M.; LaVerne, J. A. *J. Phys. Chem.* **1997**, *101*, 5828.

(18) LaVerne, J. A.; Pimblott, S. M. *J. Phys. Chem. A* **2000**, *104*, 9820.

(19) Buxton, G. V.; Greenstock, C. L.; Helman, W. P.; Ross, A. B. *J. Phys. Chem. Ref. Data* **1988**, *17*, 513.

(20) Pastina, B.; LaVerne, J. A.; Pimblott, S. M. *J. Phys. Chem. A* **1999**, *103*, 5841.

(21) Pimblott, S. M.; LaVerne, J. A. *J. Phys. Chem. A* **1998**, *102*, 2967.

(22) LaVerne, J. A.; Pimblott, S. M. *J. Phys. Chem.* **1991**, *95*, 3196.

(23) Draganic, Z. D.; Draganic, I. G. *J. Phys. Chem.* **1971**, *75*, 3950.

(24) Peled, E. *J. Phys. Chem.* **1970**, *74*, 2903.

(25) Schwarz, H. A. *J. Phys. Chem.* **1969**, *73*, 1928.

(26) Schwarz, H. A. *J. Am. Chem. Soc.* **1955**, *77*, 4960.

(27) Hug, G. L.; Wang, Y. C.; Schoneich, C.; Jiang, P. Y.; Fessenden, R. W. *Radiat. Phys. Chem.* **1999**, *54*, 559.

(28) Schuler, R. H.; Allen, A. O. *J. Chem. Phys.* **1956**, *24*, 56.

(29) Thomas, J. K.; Gordon, S.; Hart, E. J. *J. Phys. Chem.* **1964**, *68*, 1524.

(30) Solar, S.; Solar, W.; Getoff, N.; Holcman, J.; Sehested, K. *J. Chem. Soc., Faraday Trans. 1* **1985**, *81*, 1101.

(31) Solar, S.; Solar, W.; Getoff, N.; Holcman, J.; Sehested, K. *J. Chem. Soc., Faraday Trans. 1* **1984**, *80*, 2929.

(32) Solar, S.; Solar, W.; Getoff, N.; Holcman, J.; Sehested, K. *J. Chem. Soc., Faraday Trans. 1* **1982**, *78*, 2467.

(33) Patterson, L. K.; Small, R. D.; Scaiano, J. C. *Radiat. Res.* **1977**, *72*, 218.

(34) Solar, S. *J. Phys. Chem.* **1984**, *88*, 5624.

(35) Simic, M.; Ebert, M. *Int. J. Radiat. Phys. Chem.* **1971**, *3*, 259.

(36) Elliot, A. J.; McCracken, D. R.; Buxton, G. V.; Wood, N. D. *J. Chem. Soc., Faraday Trans. 1* **1990**, *86*, 1539.

(37) Rodgers, M. A. J.; Foyt, D. C.; Zimek, Z. A. *Radiat. Res.* **1978**, *75*, 296.

(38) Enomoto, K.; LaVerne, J. A.; Araos, M. S. *J. Phys. Chem. A* **2007**, *111*, 9.

(39) Lin, M. Z.; Mostafavi, M.; Muroya, Y.; Han, Z. H.; Lampre, I.; Katsumura, Y. *J. Phys. Chem. A* **2006**, *110*, 11404.

(40) Lin, M. Z.; Katsumura, Y.; He, H.; Muroya, Y.; Han, Z. H.; Miyazaki, T.; Kudo, H. *J. Phys. Chem. A* **2005**, *109*, 2847.

(41) Boilet, L.; Burdzinski, G.; Buntinx, G.; Lefumeux, C.; Poizat, O. *J. Phys. Chem. A* **2001**, *105*, 10271.

(42) Buntinx, G.; Naskrecki, R.; Poizat, O. *J. Phys. Chem.* **1996**, *100*, 19380.

(43) Poizat, O.; Buntinx, G.; Valat, P.; Wintgens, V.; Bridoux, M. *J. Phys. Chem.* **1993**, *97*, 5905.

(44) Poizat, O.; Buntinx, G.; Ventura, M.; Lautie, M. F. *J. Phys. Chem.* **1991**, *95*, 1245.

(45) Buntinx, G.; Valat, P.; Wintgens, V.; Poizat, O. *J. Phys. Chem.* **1991**, *95*, 9347.

(46) Allen, A. O. *The Radiation Chemistry of Water and Aqueous Solutions*; Van Nostrand: New York, 1961.

JP8074332